A Broadband Reflectarray Antenna using the Triangular Array Configuration

M. Mohammadirad[1], N. Komjani [1], Abdel R. Sebak[2,4], and Mohammad R. Chaharmir [3]

[1] Department of Electrical Engineering
Iran University of Science and Technology, Tehran, Iran
mohamadirad@ee.iust.ac.ir, n_komjani@iust.ac.ir

[2] Electrical and Computer Engineering
Concordia University, Montreal, Quebec, H3G 1M8, Canada
abdo@ece.concordia.ca

[3] Research Advanced Antenna Technology
Communications Research Centre Canada, Ottawa, Ontario, K2H 8S2, Canada
reza.chaharmir@crc.gc.ca

[4] PSATRI, King Saud University, Riyadh, Saudi Arabia, 11421

Abstract ─ A novel broadband reflectarray cell element is designed for use in several offset-fed reflectarray antennas based on square and triangular lattice. The proposed double-layer element consists of two stacked rectangular patches having two slots in non-radiating edges. Reflection phase curves are obtained by changing simultaneously the slot's length of top and bottom patch. The designed element exhibits a large phase-shift range in excess of 360°.This wideband cell element is designed to be used in a triangular lattice that eliminates the grating lobes for wideband reflectarrays composed of unit-cell larger than half-wavelength. Two 529-element square reflectarrays and two 518-element triangular reflectarray antennas were designed and simulated using CST and HFSS, for producing 20° and 35° off-broadside E-plane beams using a 20° offset feed. The 1-dB gain-bandwidth is about 30% at the center frequency of 14 GHz, and the maximum simulated gain is about 31 dBi which is equivalent to 51.5% aperture efficiency for a 20° off-broadside reflectarray based on triangular lattice configurations.

Index Terms ─ Cell element, gain-bandwidth, off-broadside reflectarray, triangular lattice.

I. INTRODUCTION

Traditional reflector antennas are widely used in communication systems due to their high gain and good efficiency. However, this type of antenna is not desired for some applications due to its space occupation and non-planar configuration. A new class of low profile antenna, named reflectarray antenna, has been introduced. This antenna utilizes some benefits of both reflector and phased array antennas. Due to their flat surface and printed radiating elements, there is no need for crucial mechanical manufacturing; and as a result of spatial feeding of array elements, the design complexity and high loss of feeding network are eliminated, so a higher efficiency would be achievable compared to phased arrays [1]. Other attractive properties of reflectarrays antennas are their low-cost and manufacturing simplicity compared to reflectors and phased arrays, and the possibility to generate reconfigurable features [2]. The main shortcoming is the narrowband operation compared to reflector antenna that is mainly because of intrinsic narrow

Submitted On: March 29, 2011
Accepted On: September 12, 2011

bandwidth of radiator element [3-4]. To collimate the main beam in a given direction, the elements of the reflectarray antenna must apply a specific phase-shift to the incoming spherical wave front generated by the feed. With a given feed position at a certain frequency, the required phase delay on the reflectarray surface is calculated. Different methods have been used to perform phase variation of reflectarray elements, such as variable size patches [5], slot-loaded patch [6-7], and aperture-coupled delay lines [8-9]. Besides, various kinds of structures are treated as reflectarray elements, like simple patches, loops, multi-layer configurations [10], elements with different rotation angles [11], and dielectric resonators [12]. To enhance the gain bandwidth of reflectarrays sub-wavelength patch elements have been proposed [13-14]. Also, cross and square loop elements with remarkable bandwidth and phase range properties on single-layer structure have been proposed to enhance the bandwidth of large reflectarrays [15-16].

In this paper, we utilize a triangular array configuration in designing reflectarray to eliminate the potential of grating lobes generation for wideband reflectarrays composed of a unit-cell larger than half a wavelength. Larger cell size may be applicable when we want to decrease the number of elements especially for reconfigurable reflectarray elements, which the maximum scan angle is limited by increasing the cell size. In this paper a wideband unit-cell is used. In the next sections we explain the unit-cell design and characteristics, then two reflectarrays are investigated and their simulated results are discussed.

II. CELL ELEMENT DESIGN AND SIMULATION

A. Proposed unit-cell

The presented unit-cell as shown in Fig. 1 is composed of two rectangular stacked patches on the top and bottom of RT/duroid 5880 substrate with thickness of 62mil and $\delta=0.0009$. A 2mm thick foam layer backed by the ground plane is inserted beneath the dielectric layer. Each patch has two identical slots in non-radiating edges. The phase-shift mechanism is introduced by variation of slot length. There is a possibility to make this element reconfigurable by means of a combination of MEMS switches as proposed in [17]. The scaling factor for top and bottom slot-patches is 0.6. The slot width for two patches was adjusted to the same value of 0.5mm. Also, the aspect ratio $(L_i / W_i, i = 1,2)$ for each patch is 0.8. For more reliability the phase curve sensitivity to the foam thickness was simulated. The dimensions of cell element are as follows:

$$cell\ size = 13mm, W_1 = 10mm, W_2 = 0.6W_1, L_1 = 0.8W_1, L_2 = 0.6L_1$$
$$L_{S1}: Variable, L_{S2} = 0.6L_{S1}, W_S = 0.5mm$$

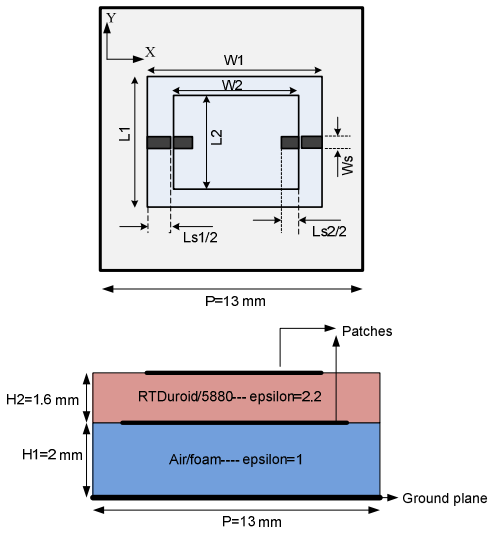

Fig. 1. Proposed unit-cell: stacked rectangular patches with two slots, top, and side view.

The reflectarray was simulated for two different lattice configurations of square and triangular using CST software [18] with periodic boundary conditions and normal plane wave excitation as shown in Fig. 2. The cell element dimensions were adjusted to achieve a linear phase-length performance. A wideband linearly phase variation with the mentioned dimensions for unit-cell was obtained where the cell size is 13mm=0.6067λ_0 at 14 GHz. Figure 3 shows the magnitude response (loss) of the proposed element at different frequencies which exhibits very low loss properties. The phase-slot's length curves for rectangular stacked patches exhibit almost linear behavior. More than 360^o phase variation was achieved by changing the slot length. Figure 4 demonstrates the reflection phase response of the element versus slot length over frequency range of 12.5-15.5 GHz, with normal plane-wave

excitation. A relatively wide linear reflection phase for this frequency range is achieved. There is no considerable difference between these two unit-cell configurations and both of them have broadband properties as reflectarray elements.

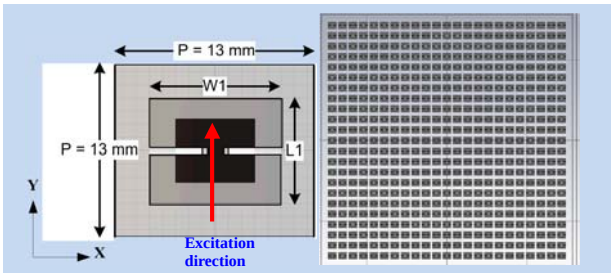

(a)

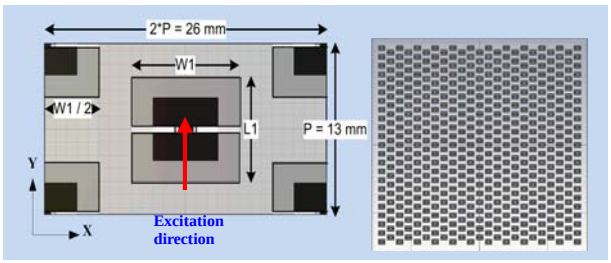

(b)

Fig. 2. Modeling of infinite array in CST for normal plane wave excitation (a) simulated unit-cell for square array (b) simulated unit-cell for triangular array.

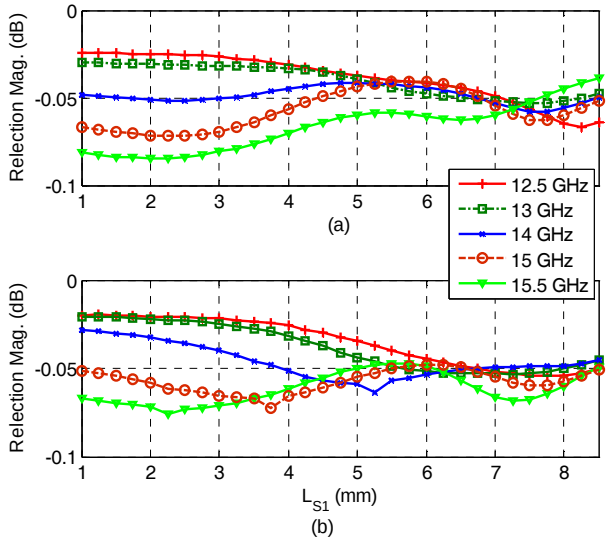

Fig. 3. Reflection magnitude (simulation) versus lower slot length at different frequencies, (a) square array (b) triangular array.

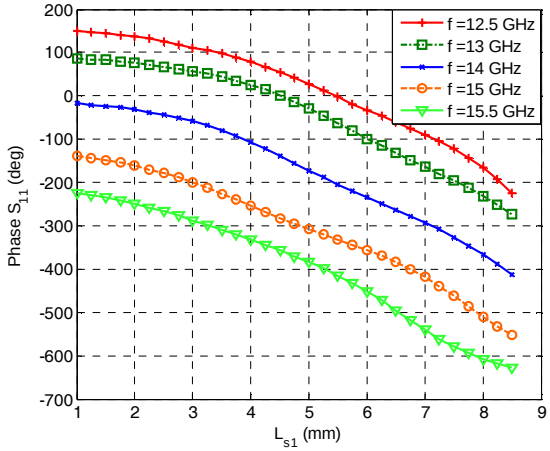

(a)

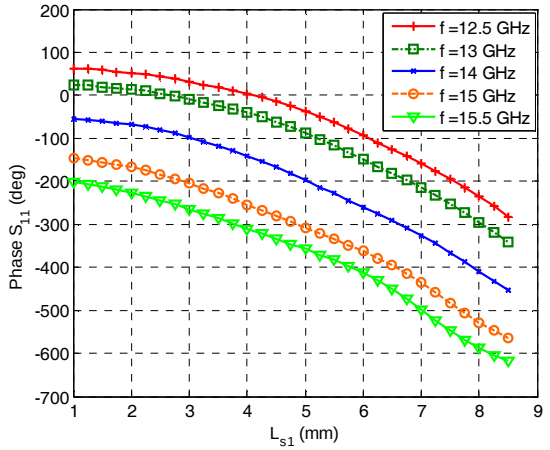

(b)

Fig. 4. Reflection phase (simulation) versus lower slot length at different frequencies, (a) square array (b) triangular array.

B. Discussion on advantages of proposed element compared with other wideband unit-cells

In classic two-layer reflectarrays e.g. the proposed element in [6], the phase variation is introduced by changing the size of two stacked patches simultaneously. Therefore, it is difficult to include the reconfigurability in such a cell element. In this work, as the phase is only controlled by the slots' lengths, it can easily be modified for dynamic phase control, e.g. using MEMS switch. Furthermore, the proposed element is etched on the top and bottom surfaces of the dielectric (RT/duroid 5880) layer in our case as compared to the multi-layer case which elements

are etched on different layers which make the fabrication more complex in this case.

On the other hand, comparing several wideband single-layer cell elements (some of them have been investigated [15-16]) with some multi-layer structures shows that more linear phase variations could be achieved when a multi-layer configuration is used since there are more parameters and space to play with in multi-layer configurations. In this design, we got the advantage of multi-layer configuration to generate a good linear phase-length curve and at the same time make the fabrication complexity something between single-layer and multi-layer configurations.

III. REFLECTARRAY DESIGN AND SIMULATION

All the reflectarrays, designed in this paper are offset-fed with a dimension of 30cm×30cm and *F/D=0.9* as shown in Fig. 5. The feed location was calculated to provide 10 *dB* amplitude tapering on the aperture of the reflectarray. There are 23 elements in each direction with the cell size of 13mm×13mm.

The phase distribution on reflectarray surface is given by:

$$\phi_R = k_0\left(d_i - \left(x_i\cos\varphi_b + y_i\sin\varphi_b\right)\sin\theta_b\right), \qquad (1)$$

where (φ_b, θ_b) denote the main beam direction, d_i is the distance between the source point and $i-$th element, and (x_i, y_i) are the coordinates of the element i. To realize the required phase-shift on the reflectarray surface the length of slots were determined using the phase curve of previous section at center frequency of 14 GHz. After applying these lengths, the reflectarray is modeled by the full-wave electromagnetic software CST Microwave Studio and Ansoft HFSS to validate the design. In all the simulations, a linearly polarized waveguide horn antenna was used to illuminate the reflectarray with the E-plane and H-plane patterns are approximated by $\cos^{12}\theta$, as shown in Fig. 6.The feed which is fed by *WR62* waveguide has an aperture size of 55.8mm × 43.9mm, and length=73.3mm. As an example, the calculated phase distribution at 14 GHz on a square lattice reflectarray to produce a 35° off-broadside beam is shown in Fig. 7.

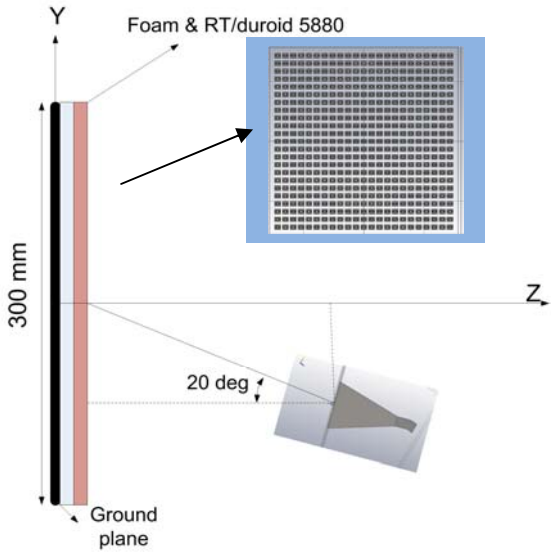

Fig. 5. Schematic view of the reflectarray.

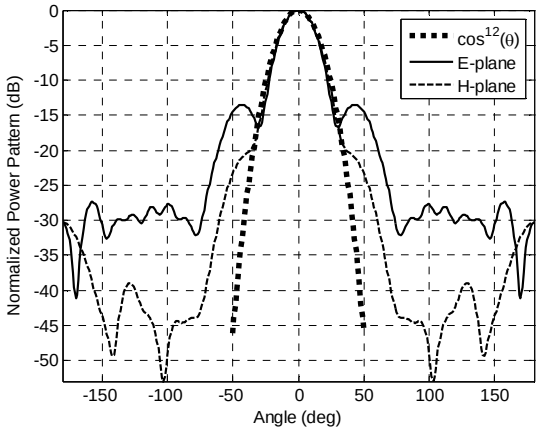

Fig. 6. E-plane and H-plane patterns of the feed horn and their approximation.

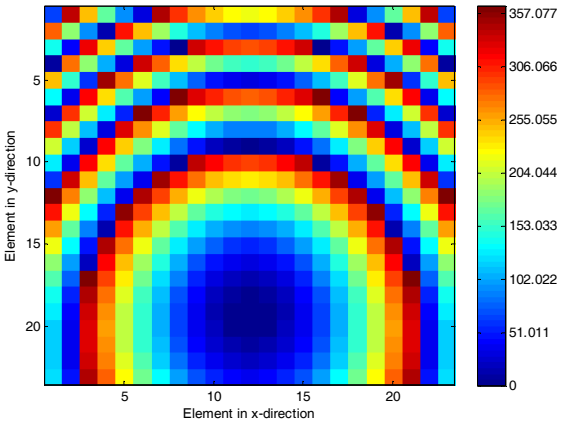

Fig. 7. Phase distribution on square lattice for 35° off-broadside offset-fed reflectarray, at 14 GHz.

Four offset-fed reflectarrays with square and triangular lattices are designed for producing 20^o and 35^o off-broadside main beams. First, these reflectarrays are compared from the computational cost point of view then a discussion will be carried out on their radiation properties and bandwidth performance in the next section. Two commercial software CST [18] and HFSS [19] were used for simulating these reflectarrays. Ansoft HFSS software is based on a three-dimensional full-wave finite element (FE) method for solving the differential form Maxwell's equations in the frequency-domain. Ansoft HFSS software automatically converts the whole structure into a finite element mesh which consists of a large number of very small 3D tetrahedral shapes. Typically, meshing or discretizing operations done by Ansoft HFSS is very coarse in almost the whole structure and it is very fine at some regions which need more accuracy such as near wave port, metallic edges or discontinuities. After finalizing the mesh operation of the whole structure, the solution process starts with two-dimensional (2D) port solutions then followed by the field solution of the full 3D problem. The program exploits the computed 2D fields on ports to be used as boundary conditions to solve the 3D fields of the whole structure. The other simulation software is CST Microwave Studio (MWS). CST MWS is based on the finite integration technique (FIT) which is equivalent to FDTD. Unlike the FE method, FIT is a time-domain numerical technique for solving Maxwell's equations. Using the function of the parametric study in both Ansoft HFSS and CST MWS simulation programs, we can tune and optimize the structure physical parameters to improve the design before going to fabrication process. CST MWS has different kinds of solvers not only transient solver but also frequency domain solver, Eigen mode solver and integral equation solver. There are several differences between these two CAD tools in defining the structure, solution setup, and solution methods. For convergence purposes, the main factors that may be considered in CST and HFSS are mesh properties and solution setup, respectively.

Numerical simulations have been carried out using a computer with Intel i7-920 (8 cores) CPU and 12 GB of RAM. Considering the available hardware, the complete structure (horn in front of the reflectarray) is completely simulated in CST. However, for simulating the structure in HFSS, the feed horn was simulated separately and its far-field results were used as excitation for the reflectarray antenna. In this simulation the coupling between the horn feed and reflectarray is not taken into account which is negligible for offset-fed configuration [2]. In the considered 11-18 GHz band with 0.25 GHz step, for more solution accuracy over the wide simulating band and reliable results it is better to define more than one solution setup in HFSS. The convergence criterion in CST and HFSS are different.

In CST, the convergence is controlled with a parameter called "accuracy". The accuracy setting in CST defines the steady-state monitor. It influences the duration of the simulation. It is a value for the accuracy of the frequency domain signals that are calculated by Fourier transformation of the time domain signals. To get a value for the accuracy, the amplitudes of the time signals as well as the total energy inside the calculation domain are used. During the simulation, the total energy value is frequently calculated and related to the maximum energy that has been monitored thus far [18]. In our simulations this parameter was set to -30 dB to insure an almost damped reflected time domain signal at the waveguide input port.

In HFSS, the convergence is defined in terms of "maximum delta energy". It is a stopping criterion for the adaptive solution when ports have not been defined as applied to our case where the excitation is an incident field. The error is a measure of the solution's accuracy. This convergence criterion is based on the change in a computed energy term. As the solution converges, this term approaches constant value and the delta energy approaches zero. To minimize the delta energy, the system refines the mesh in tetrahedral shapes that have the largest error. The delta energy that appears on screen represents the delta energy for all tetrahedral [19]. In our simulations this parameter was set to 0.02 due to memory limitation and to have an acceptable accuracy.

A comparison between CST and HFSS simulations can be useful from the computational

cost point of view, as presented in Table 1. As compared in Table 1, considering the available memory, time, and desired bandwidth the reasonable choice for simulating a wideband reflectarray seems to be CST compared to HFSS. Due to a different meshing scheme, the number of mesh cells is not comparable to each other as shown in the last column of Table 1.

Table 1: Comparison of HFSS and CST simulations

Reflectarray lattice and main beam direction	Software	Memory usage (GB)	Total simulation time (hrs:mins)	Number of mesh cells
Triangular array 20°	CST 2010	9.1	6:40	66719526 hexahedral
	HFSS v.12	10.4	11:36	452347 tetrahedral
Triangular array 35°	CST 2010	8.8	6:56	63702060 hexahedral
	HFSS v.12	9.4	5:20	435721 tetrahedral
Square array 20°	CST 2010	8.8	6:58	64627200 hexahedral
	HFSS v.12	10.7	9:48	487161 tetrahedral
Square array 35°	CST 2010	9	7:31	66549120 hexahedral
	HFSS v.12	8.4	5:06	409539 tetrahedral

To demonstrate the agreement between the CST and HFSS results, the radiation patterns at 15 GHz and 16 GHz for two square arrays are compared in Fig. 8 and Fig. 9, respectively. Therefore, with respect to this similarity and for the sake of brevity, the obtained radiation pattern from CST is merely compared for the triangular and square lattice as provided in the next section.

IV. THEORETICAL ANALYSIS AND DISCUSSION ON SIMULATION RESULTS

A. Grating lobe problem

With scanning, lobes that were originally in imaginary space may move into real space if the element spacing is greater than $\lambda/2$. As the array is scanned away from broadside, each grating lobe (in $\sin\theta$ space, *i.e.* $\varphi = 90^o$) will move a distance equal to the sine of the angle of scan and in a direction determined by the plane of scan [20]. To ensure that no grating lobes enter real space, the element spacing must be chosen so that for the maximum scan angle θ_0 the movement of a grating lobe by $\sin\theta_0$ does not bring the grating lobe into real space which is expressed as follows:

$$\frac{s}{\lambda} < \frac{1}{1+|\sin\theta_0|}, \qquad (2)$$

where ***s*** is the cell size. The highest frequency that satisfies this condition is 17.2 GHz for $\theta_0 = 20^o$ and 14.65 GHz when $\theta_0 = 35^o$.

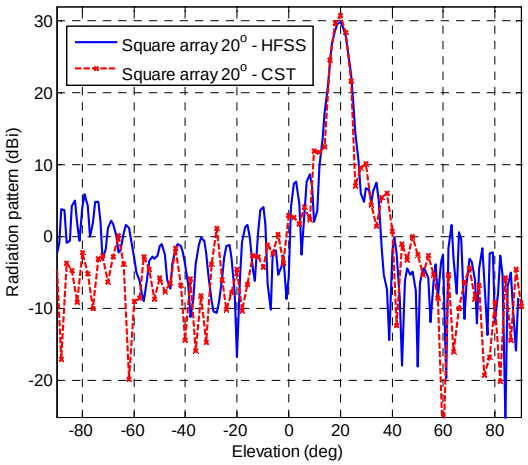

Fig. 8. Radiation pattern at 15 GHz for square array 20°, CST, and HFSS comparison.

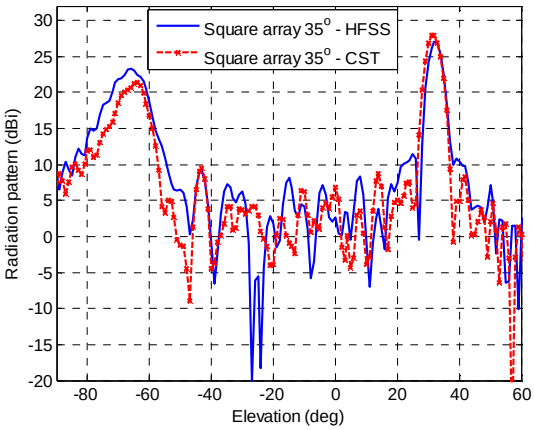

Fig. 9. Radiation pattern at 16 GHz for square array 35°, CST and HFSS comparison.

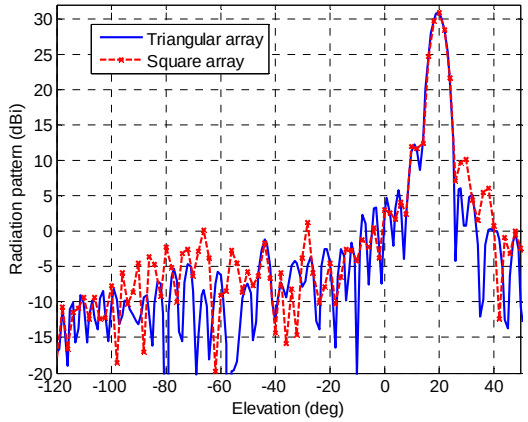

(a)

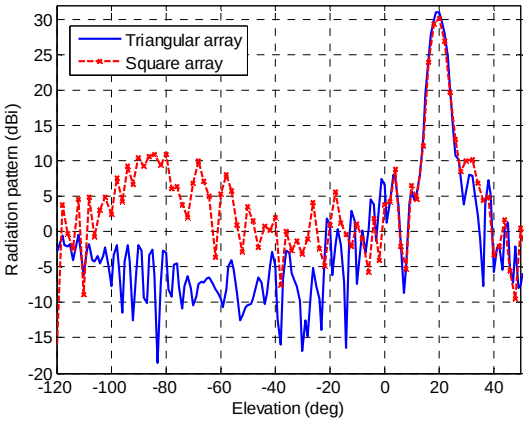

(b)

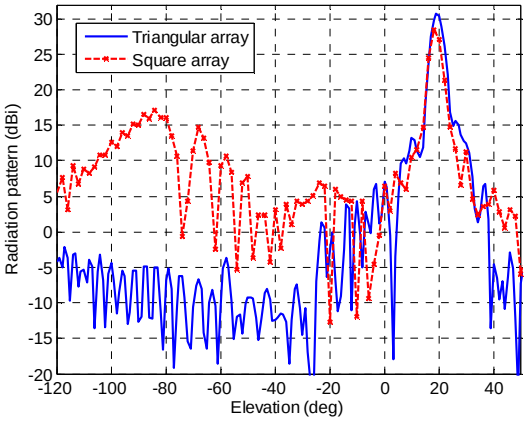

(c)

Fig. 10. Comparison of 20° off-broadside reflectarray radiation patterns (E-plane) at (a) 14 GHz (b) 16 GHz (c) 17 GHz.

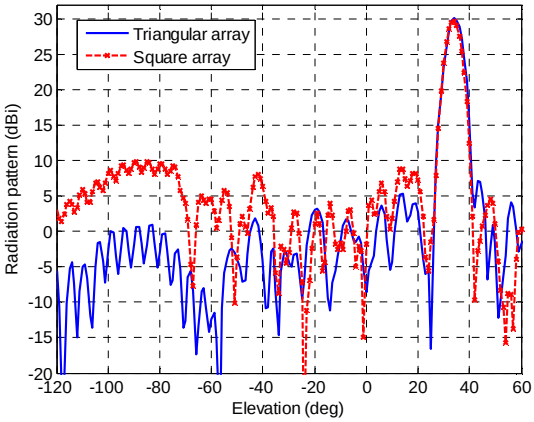

(a)

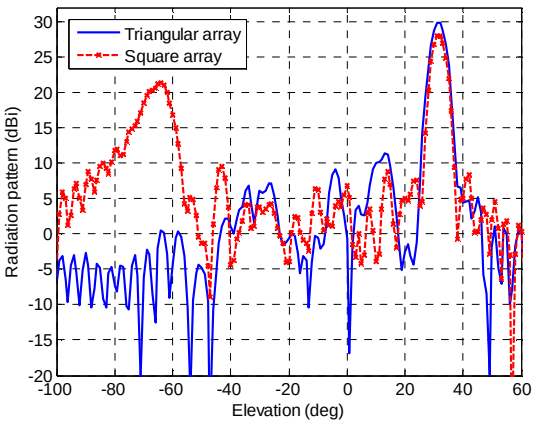

(b)

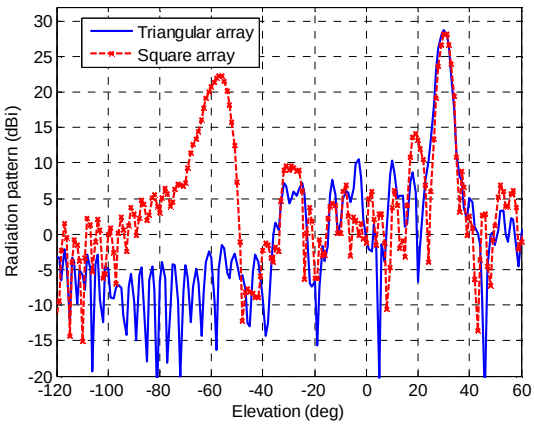

(c)

Fig. 11. Comparison of 35° off-broadside reflectarray radiation patterns (E-plane) at (a) 14 GHz (b) 16 GHz (c) 17 GHz.

B. Simulation results: radiation patterns

The simulated radiation patterns in E-plane at 14 GHz, 16 GHz, and 17 GHz for the reflectarray with main beam at *20°* and *35°* are shown in Fig. 10 and Fig. 11, respectively.

Regarding the above analysis, it can be seen in Fig. 10 that for *20°* main beam, the radiation

patterns of square and triangular lattices are appropriate; although the grating lobe is appearing at 17 GHz for square lattice.

On the other hand, as demonstrated in Fig. 11 when the main beam is directed to *35°* off-broadside, the grating lobe level for the square lattice is significantly higher than the triangular lattice due to the grating lobe generated in the square lattice reflectarray. It is to be noted that whereas the main beam is scanned in E-plane, consequently the grating lobe in H-plane does not exist and therefore most of results are presented in E-plane ($\varphi=90^o$). However, regarding the $\pm45^o$ plane, there are some side lobes but in much lower level than the grating lobe in E-plane. Also, radiation patterns at $\varphi=45^o$ and $\varphi=0^o$ (H-plane) have been compared for the square and triangular lattices at 17 GHz, as shown in Fig. 12.

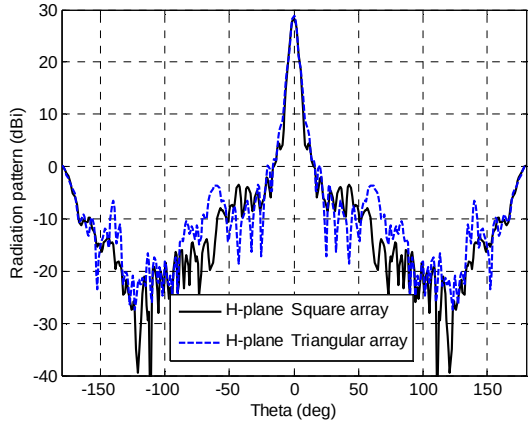

(a)

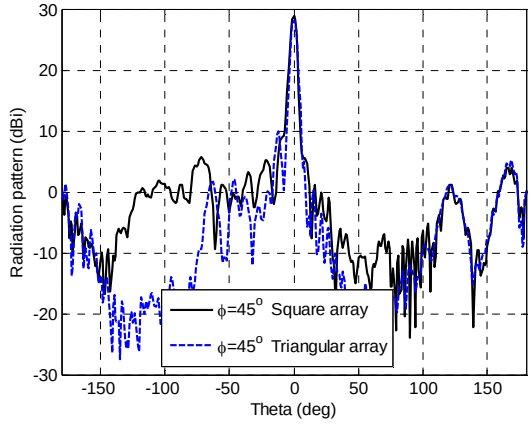

(b)

Fig. 12. Cut-plane patterns at 17 GHz, 35° off-broadside reflectarray, (solid) square lattice, (dashed) triangular lattice (a) H-plane, (b) 45° plane.

Figure 13 shows the 3D radiation patterns for 35° off-broadside reflectarray designed on triangular configuration at 17GHz.

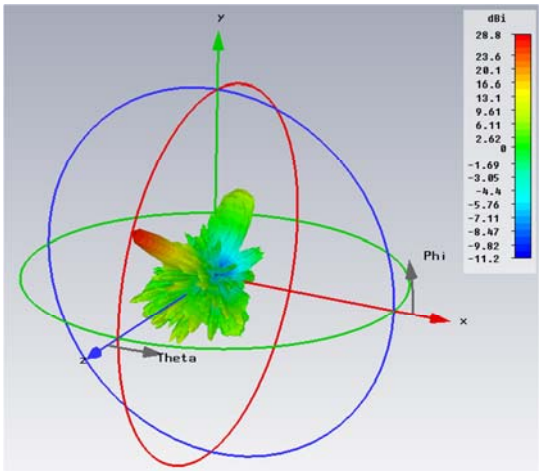

Fig. 13. 35° off-broadside 3D radiation pattern of triangular array at 17 GHz.

C. Simulation results: gain curves

The calculated gain using CST and HFSS are compared in this section. The simulated gain versus frequency for four reflectarrays is shown in Fig. 14 to Fig. 17. Comparing these figures provides a better insight into the bandwidth performance of the reflectarray based on the triangular and square lattices.

Refering to radiation patterns shown in Fig. 10, the gain curves of Fig. 14 and Fig. 15 are obtained. As it can be seen for both CST and HFSS results the triangular reflectarray with main beam at *20°* exhibits a simulated *1-dB* gain-bandwidth of about 30% which is higher than the square array's one. However, for *20°* square reflectarray the grating lobe is slightly observed at higher frequencies.

Similarly, refering to radiation patterns presented in Fig. 11, the gain curves of Fig. 16 and Fig. 17 are derived. Comparing the gain results in these figures shows that the triangular reflectarray with main beam at *35°* exhibits a simulated *1-dB* gain-bandwidth of about 3.5 GHz which is much higher than the square array. In the case of square lattice for *35°* main beam, a sharp drop in gain can be seen for frequencies higher than 14.5 GHz, which is mainly due to the grating lobe. However, using the triangular array configuration, the grating lobe is eliminated and consequently gain

bandwidth increases due to a gain increment at higher frequencies. In other words, using triangular array leads to compensation and stability of gain curve especially at upper frequencies of operation. Furthermore, the grating lobe problem can be untangled in this way particularly when a large angle of scan is needed for a broadband reflectarray.

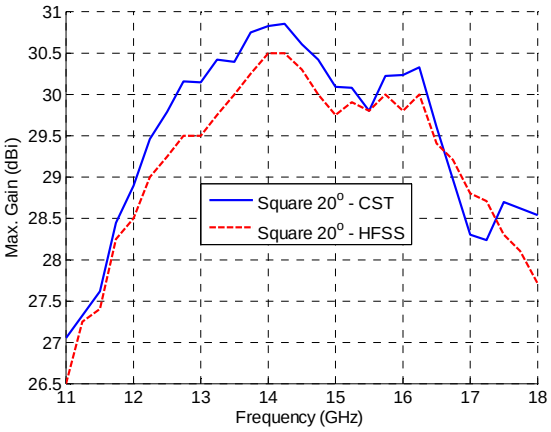

Fig. 14. Gain curve of reflectarray with square lattice for main beam at 20°.

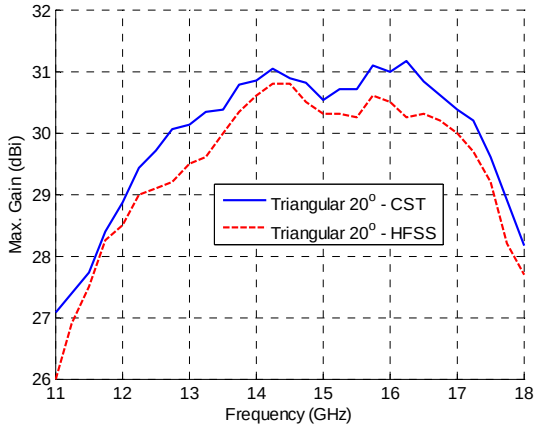

Fig. 15. Gain curve of reflectarray with triangular lattice for main beam at 20°.

V. CONCLUSION

A novel broadband reflectarray cell element is presented. This unit-cell was used for designing several 30 cm × 30 cm offset-fed reflectarrays at Ku-band. A 20° offset-fed configuration was chosen to produce 20° and 35° off-broadside main beam. Whereas, the element spacing is greater than $\lambda/2$ and the main beam is scanned away from broadside the triangular array lattice is utilized to avoid grating lobe issue at higher frequencies. Results showed that we can design reflectarray based on triangular array where the unit cell size is more than half wavelength, especially when a large angle of scan is required in a broadband reflectarray. Comparing CST and HFSS results showed that CST is faster than HFSS for simulating wideband reflectarrays. The simulated results show a significant improvement in the radiation pattern and gain bandwidth of the reflectarray, when we utilize the advantages of the triangular lattice in designing reflectarray rather than the conventional square one, especially for main beam at 35°. Also, the triangular reflectarray with main beam at 20° exhibits the simulated 1-dBgain-bandwidth of 30% which is considerable for a reflectarray antenna.

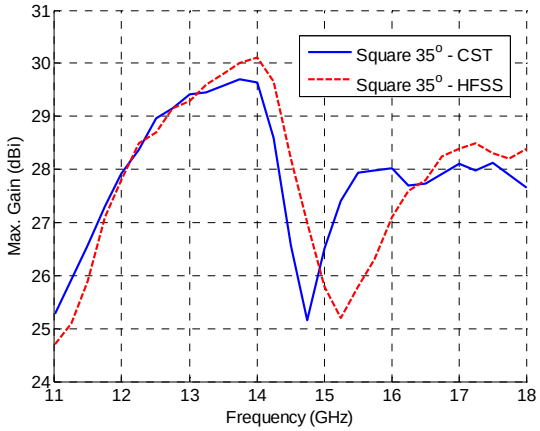

Fig. 16. Gain curve of reflectarray with square lattice for main beam at 35°.

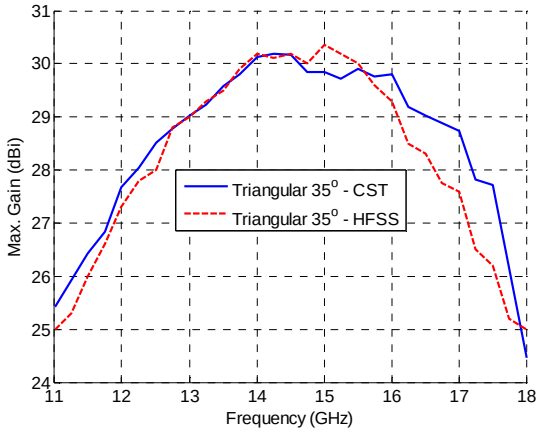

Fig. 17. Gain curve of reflectarray with triangular lattice for main beam at 35°.

ACKNOWLEDGMENT

This work has been partially supported by the Iran Telecommunication Research Center (Research Institute for ICT - ITRC).

REFERENCES

[1] D. M. Pozar, S. D. Targonski, and H. D. Syrigos, "Design of Millimeter-Wave Microstrip Reflectarray," *IEEE Transactions on Antennas and Propagation*, vol. 45, no. 2, pp. 286–295, Feb. 1997.

[2] J. Huang and J. A. Encinar, Reflectarray Antennas, New York: IEEE Press, 2008.

[3] M. Riel and J.-Jacques Laurin, "Design of an Electronically Beam Scanning Reflectarray Using Aperture-Coupled Elements," IEEE Transactions on Antennas and Propagation, vol. 55, no. 5, pp. 1260-12661, May 2007.

[4] B. Devireddy, A. Yu, F. Yang, and A. Z. Elsherbeni, "Gain and Bandwidth Limitations of Reflectarrays," Applied Computational Electromagnetic Society (ACES) Journal, vol. 26, no. 2, pp. 170–178, Feb. 2011.

[5] D. M. Pozar, "Bandwidth of Reflectarray," Electron. Lett., vol. 39, no. 21, pp. 1490–1491, Oct. 2003.

[6] J. A. Encinar, "Design of Two-Layer Printed Reflectarrays using Patches of Variable Size," IEEE Transactions on Antennas and Propagation, vol. 49, no. 10, pp.1403–1410, Oct. 2001.

[7] D. Cadoret, A. Laisne, R. Gillard, and H. Legay, "A New Reflectarray Cell Using Microstrip Patches Loaded with Slots," Microwave and Optical Technology Letters, vol. 44, no. 3, pp. 270–272, Feb. 2005.

[8] M. Bozzi, S. Germani, and L. Perregrini, "A Figure of Merit for Losses in Printed Reflectarray Elements," IEEE Antennas and Wireless Propagation Letters, vol. 3, pp. 257-260, 2004.

[9] E. Carrasco, M. Arrebola, J. A. Encinar, and M. Barba, " Demonstration of a Shaped Beam Reflectarray Using Aperture-Coupled Delay Lines for LMDS Central Station Antenna," IEEE Transactions on Antennas and Propagation, vol. 56, no. 10, pp. 3103-3111, Oct. 2008.

[10] J. Encinar and J. A. Zornoza, "Broadband Design of a Three-Layer Printed Reflectarray," IEEE Transactions on Antennas and Propagation, vol. 51, no. 7, pp. 1662–1664, Jul. 2003.

[11] J. Huang, and R. J. Pogorzelski, "A Ka-band Microstrip Reflectarray with Elements Having Variable Rotation Angles," IEEE Transactions on Antennas and Propagation, vol. 46, no. 5, pp. 650–656, May 1998.

[12] M. Ab-Elhady, S. H. Zainud-Deen, A. A. Mitkees, and A. A. Kishk, "X-Band Linear Polarized Aperture-Coupled DRA Reflectarray," Microwave and Millimeter Wave Technology (ICMMT), 2010 International Conference, pp. 1042 – 1044, May 2010.

[13] P. Nayeri, F. Yang, and A. Z. Elsherbeni, "A Broadband Microstrip Reflectarray using Sub-Wavelength Patch Elements," IEEE APS/URSI, pp. 1-4, 2009.

[14] P. Nayeri, F. Yang, and A. Z. Elsherbeni, "Broadband Reflectarray Antennas using Double-Layer Subwavelength Patch Elements," IEEE Antennas and Wireless Propagation Letters, vol. 9, pp. 1139-1142, 2010.

[15] M. R. Chaharmir, J. Shaker, N. Gagnon, and D. Lee, "Design of Broadband, Single Layer Dual-Band Large Reflectarray Using Multi Open Loop Elements," IEEE Transactions on Antennas and Propagation, vol. 58, no. 9, Sept. 2010.

[16] M. R. Chaharmir, J. Shaker, and H. Legay, "Broadband Design of a Single Layer Large Reflectarray Using Multi Cross Loop Elements," IEEE Transactions on Antennas and Propagation, vol. 57, no. 10, pp. 3363–3366, Oct. 2009.

[17] H. Rajagopalan, Y. Rahmat-Samii, and W. A. Imbriale, "RF MEMS Actuated Reconfigurable Reflectarray Patch-Slot Element," IEEE Transactions on Antennas and Propagation, vol. 56, no. 12, pp. 3689–3699, Dec. 2008.

[18] CST Computer Simulation Technology, "3D EM Simulation Software," Online: http://www.cst.com

[19] Ansoft HFSS, "The 3D, electromagnetic, finite-element simulation tools for high-frequency design," [Online]. Available: http://www.ansoft.com

[20] M. I. Skolnik, Radar Handbook. McGraw Hill, 2nd Ed., 1990.

Mohammad Mohammadirad received his B.S and M.S. degree from Iran University of Science and Technology in 2004 and 2007, respectively, both in Electrical Engineering. He is currently working toward the Ph.D. degree at Iran University of Science and Technology. His research interests include reflectarray antennas, reflector antennas, UWB antenna, array antenna design, development, implementation and measurement.

Nader Komjani received his BSc., MSc. and PhD. degree all in Electrical Engineering from Iran University of Science and Technology, Iran, in 1988 and 1991, and 2000, respectively. He is currently the associate professor with Iran University of Science and Technology.
He has taught microstrip antenna, communication systems, advanced engineering mathematics and electromagnetic courses since 1998. His research interests are in the areas of UWB and multiband microstrip antennas, numerical methods in electromagnetic, phased array antennas and passive and active microwave systems.

Abdel-Razik Sebak received the B.Sc. degree (with honors) in Electrical Engineering from Cairo University, Egypt, in 1976 and the B.Sc. degree in Applied Mathematics from Ein Shams University, Egypt, in 1978. He received the M.Eng. and Ph.D. degrees from the University of Manitoba, Winnipeg, MB, Canada, in 1982 and 1984, respectively, both in Electrical Engineering. From 1984 to 1986, he was with the Canadian Marconi Company, Kanata, Ontario, working on the design of microstrip phased array antennas. From 1987 to 2002, he was a Professor in the Electrical and Computer Engineering Department, University of Manitoba, Winnipeg. He is currently a Professor of Electrical and Computer Engineering, Concordia University, Montreal. His current research interests include phased array antennas, computational electromagnetics, integrated antennas, electromagnetic theory, interaction of EM waves with new materials and bio-electromagnetics. Dr. Sebak received the 2007-2008 Faculty of Engineering, Concordia University double Merit Award for outstanding Teaching and Research. He has also received the 2000 and 1992 University of Manitoba Merit Award for outstanding Teaching and Research, the 1994 Rh Award for Outstanding Contributions to Scholarship and Research in the Applied Sciences category, and the 1996 Faculty of Engineering Superior Academic Performance. Dr. Sebak has served as Chair for the IEEE Canada Awards and Recognition Committee (2002-2004) and IEEE Canada CONAC (1999-2001). He has also served as Chair of the IEEE Winnipeg Section (1996-97). He was the Technical Program Co-Chair (2006) and served as the Treasurer (1992, 1996, and 2000) and Publicity Chair (1994) for the Symposium on Antenna Technology and Applied Electromagnetics (ANTEM). Dr. Sebak has also served as Chair (1991-92) of the joint IEEE AP/MTT/VT Winnipeg Chapter. He received, as the Chapter Chair, the 1992 IEEE Antennas and Propagation Society Best Chapter Award. He is a Fellow Member of the IEEE, and a member of the International Union of Radio Science Commission B.

Mohammad Reza Chaharmir received the B.Sc. degree (with honors) in Electrical Engineering from K. N. Toosi University of Technology, Tehran, Iran, in 1993, the M.Sc. degree in Electrical Engineering from Amir Kabir University of Technology, Tehran, in 1996, and the Ph.D. degree in electrical engineering from the University of Manitoba, Winnipeg, MB, Canada, in 2004.
He has been a Research Scientist at the Communications Research Centre (CRC), Ottawa, ON, Canada, since 2005. He has also been an Adjunct Professor at Concordia University, Montreal, Canada, since 2005. His research interests and activities include periodic structures, reflectarray antennas, FSS, band gap photonic, metamaterials and antenna beam scanning.